

# Shear Rate Dependence of Viscosity and First Normal Stress Difference of LCP/PET Blends at Solid and Molten States of LCP

S. A. R. Hashmi,<sup>1</sup> Takeshi Kitano<sup>2</sup>

<sup>1</sup>Regional Research Laboratory (CSIR), Bhopal 462026, India

<sup>2</sup>National Institute of Advanced Industrial Science and Technology (AIST), Research Centre of Macromolecular Technology, 1-1-1, Higashi, Tsukuba, Ibaraki 305-0046, Japan

Received 18 August 2005; accepted 23 March 2006

DOI 10.1002/app.24642

Published online in Wiley InterScience (www.interscience.wiley.com).

**ABSTRACT:** The liquid crystalline polymer (LCP) and polyethylene terephthalate (PET) were blended in an elastic melt extruder to make samples having 20, 40, 60, 80, and 100 wt % of LCP. Morphology of these samples was studied using scanning electron microscopy. The steady state shear viscosity ( $\eta$ ), dynamic complex viscosity ( $\eta^*$ ) and first normal stress difference ( $N_1$ ) were evaluated and compared at two temperatures: 265°C, at which LCP was in solid state, and 285°C, at which LCP was in molten state. The PET was in molten state at both the temperatures. The shear viscosity of the studied blends displayed its dependence on composition

and shear rate. A maxima was observed in viscosity versus composition plot corresponding to 80/20 LCP/PET blend. The  $N_1$  increased with LCP loading in PET and with the increased asymmetry of LCP droplets. The  $N_1$  also varied with the shear stress in two stages; the first stage demonstrated elastic deformation, whereas second stage displayed dominant plastic deformation of LCP droplets. © 2007 Wiley Periodicals, Inc. *J Appl Polym Sci* 104: 2212–2218, 2007

**Key words:** LCP/PET blend; rheological properties; viscosity; first normal stress difference; shear rate

## INTRODUCTION

The liquid crystalline polymers (LCPs) are known for high performance engineering materials with high strength and stiffness, high chemical resistance, good dimensional stability, and low linear thermal expansion coefficient. They are blended with other polymers to produce composites with superior mechanical properties at reasonably low cost.<sup>1,2</sup> The LCPs are also known as processing aid for reducing the viscosity of thermoplastic polymers during compounding. They consist of repeating stiff mesogenic (liquid crystalline) monomer units, which are incorporated either in the main-chain or in the side chain of a polymer backbone. The anisotropic mesogenic moieties of LCP become oriented along the flow field within isotropic thermoplastic polymer liquid during melt processing of polymers and lead to the formation of fine fibrils at an appropriate range of LCP concentration under certain processing conditions and reinforce the thermoplastics, giving rise to the development of *in situ* polymer composites.<sup>1–10</sup> LCPs display different morphologies when mixed with other thermoplastics such as polyethylene terephthalate (PET).<sup>7,10</sup> The shape of dispersed LCP varies from spherical, elliptical, layered to

fibrous shape and depends upon the volume fraction of LCP, viscosity, imposed shear conditions, interfacial tensions, etc.<sup>4–10</sup> The reduction in viscosity of blends having LCP as one of the components has been reported in most of the studies related to LCP/PET blend; however the increase in viscosity of LCP/PET blends at 250, 260, 270°C at shear rates less than  $100 \text{ s}^{-1}$  has rarely been discussed.<sup>10</sup> In the present investigation the morphology of different blends, shear rate dependence of viscosity, and first normal stress difference ( $N_1$ ) of LCP/PET blends at two different temperatures each one at below and above the melting temperature of LCP with varying blend composition are reported and discussed.

## MATERIALS AND METHODS

The liquid crystalline polymer Vectra A 950 of Polyplastics, Japan was used in this study, which is a commercial copolyester having 73 mol % of *p*-hydroxybenzoic acid and 27 mol % of 2-6-hydroxynaphtioic acid (HNA). The polyethylene terephthalate (PET) was a commercial product SA1206 of Unitika, Japan. Both polymers were dried in an oven at 90°C for 14 h and then at 150°C for 4 h before processing. The composition was varied as 20, 40, 60, 80, and 100 wt % of LCP in LCP/PET blend. Blending was carried out in an elastic melt extruder at 285°C. The elastic melt extruder works on the Weissenberg principle.<sup>11</sup> The material was fed

Correspondence to: S. A. R. Hashmi (sarhashmi@rediffmail.com).

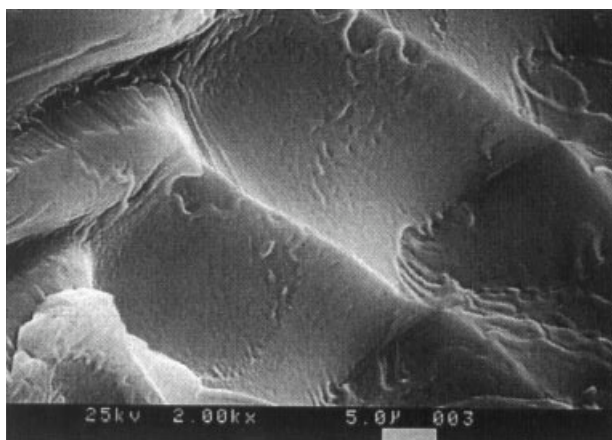


**Figure 1** SEM of fractured surface of extruded PET.

directly into the shearing zone, which is built by the rotor and stator. The effective rotor diameter is 14 cm. The extruded material was quenched in water at 12°C and was immediately cut by pelletizer to a 5 mm length. The pellets were dried in an air-circulating oven at 75°C for 12 h. The process was repeated once to achieve better mixing. A weighed amount of pellets was placed in the mold. The material was compressed between the hot plates for 3 min under 5 MPa pressure at 265°C. The mold was then cooled immediately under the same pressure by circulating water at 12°C and sheets were prepared. These sheets were cut to disc shape for tests by using a sawing machine. These discs were tested on a cone plate type rheometer (radius,  $R = 1.25$  cm), from Nihon Rheology Ki-Ki Co. The shear stress  $\sigma_{12}$ , shear viscosity  $\eta$ , and first normal stress difference  $N_1$  were calculated using following relations:<sup>12</sup>

$$\sigma_{12} = 3T/2\pi R^2$$

$$\eta = \sigma_{12}/\dot{\gamma}'$$

$$N_1 = 2F/\pi R^2$$

where torque  $T$  and thrust  $F$  acting on cone were measured at different shear rates  $\dot{\gamma}'$ .

The absolute value of complex viscosity,  $|\eta^*|$  was calculated from storage modulus  $G'$  and loss modulus  $G''$  values, which are determined at different angular frequencies,  $\omega$ , using oscillatory angle 4°, and at 100% strain amplitude at two different temperatures as per following relation<sup>13</sup>

$$|\eta^*| = [(G'/\omega)^2 + (G''/\omega)^2]^{1/2}$$

The scanning electron microscope was used to observe the fractured surfaces of LCP, PET, and LCP/PET blends extruded through a capillary of 1 mm diameter and 30 mm length.

## RESULTS AND DISCUSSIONS

### Morphology

The melt blended immiscible polymer blends generally exhibit the complicated morphology that depends upon volume fraction, viscosity-difference of constituent polymers, interfacial tension, processing condition, etc. The size and shape of dispersed phase is governed by the viscoelastic effects balanced by the interfacial tension.<sup>14,15</sup> The LCPs are incompatible with the thermoplastics because the melt of LCP displays anisotropy, whereas the latter show isotropy. The nematic LCPs can easily be oriented parallel to the direction of flow in anisotropic melt state and can form fibrous structure.<sup>5-7</sup> The cryogenic fractured surfaces of PET, LCP, and LCP/PET blends are shown in Figure 1, Figure 2, and Figure 3, respectively. The morphological features of PET and LCP can be distinguished easily as shown in Figure 1 and Figure 2. PET shows smooth wavy surface whereas LCP is characterized with fibrous morphology. The fibers were formed in LCP while passing through a capillary of 30 mm length at 285°C. Interesting features were observed in LCP/PET blends as shown in Figure 3(a), 3(b), 3(c), and 3(d). Several cavities were observed in the fractured surface of 20:80 LCP/PET blend, suggesting spherical particles of LCP distributed in PET matrix as shown in Figure 3(a). Only a few spherical particles were found to be retained on the surface. The cavities are smooth and there is no evidence of bonding between PET and LCP. Figure 3(b) is slightly different than Figure 3(a) as the layers and fibers were also observed along with few cavities. The formation of layers and fibers may be attributed to the increased number of LCP particles with the increased LCP content and possible coalesce of these particles combined with the sheared flow inside the capillary. A further increase in LCP content in the blend modifies the morphology as shown in Figure 3(c) wherein the thin layers can be observed.

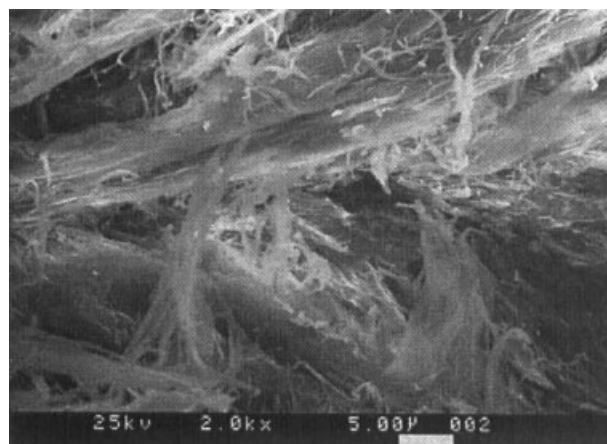


**Figure 2** SEM of fractured surface of extruded LCP.

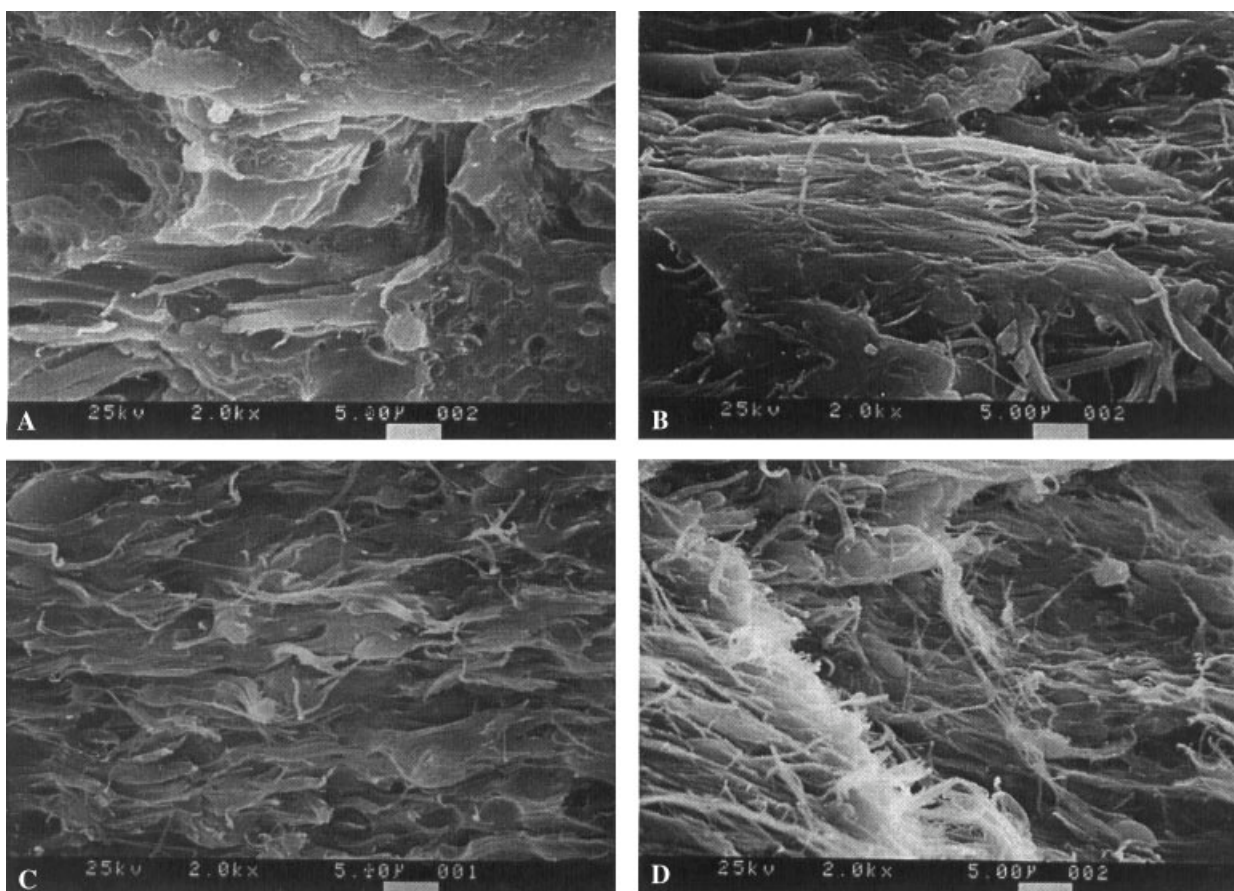


**Figure 3** SEM of fractured surface of extruded LCP/PET blend: (a) 20/80, (b) 40/60, (c) 60/40, and (d) 80/20.

The morphology of 80 : 20 LCP/PET blend as shown in Figure 3(d) resembles that of LCP. In this sample morphological features of LCP dominate over that of PET. The morphology of LCP/PET samples that were prepared under identical process conditions strongly exhibits the composition dependency.

### Shear viscosity

Figure 4 shows plots between the viscosity and composition of LCP/PET blends at two different temperatures; 265 and 285°C at different shear rates. Filled symbols are used to represent viscosity value at temperature 265°C and unfilled symbols represent viscosity corresponding to 285°C. Viscosity data could not be obtained for sample containing 80 vol % of LCP in PET at 265°C. Melt temperature of LCP was higher than 265°C and therefore shear rate dependent viscosity data related to LCP is absent in this plot. The effect of shear rate can also be seen in this plot wherein the observed shear viscosity was shear dependent; for example at 265°C, a 60 : 40 LCP/PET blend shows a viscosity of 13.7 kPa s at shear rate of 0.15 s<sup>-1</sup>, which decreased to 6.8 kPa s corresponding to a shear rate of 0.60 s<sup>-1</sup>. The decrease in shear viscosity with increased shear rate is commonly observed in most of polymers

and their blends, and generally referred as shear thinning phenomenon. The curves represented by continuous lines and distinguished by the filled and unfilled symbols can be compared. They represent viscosities at same shear rates but at different temperatures. The

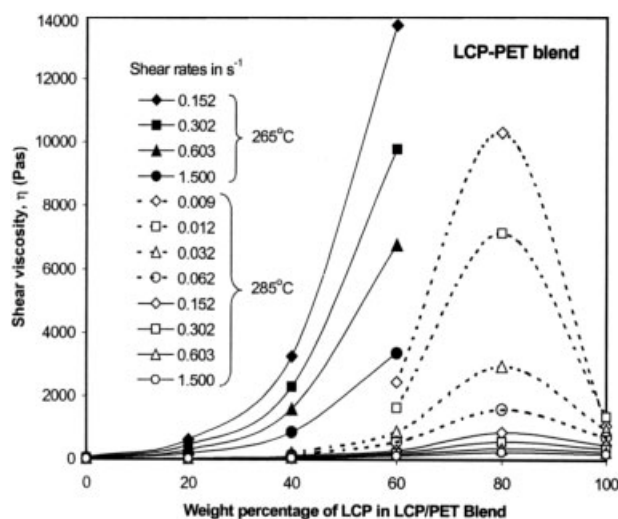


**Figure 4** Plots between the viscosity and composition of blends at different shear rates.



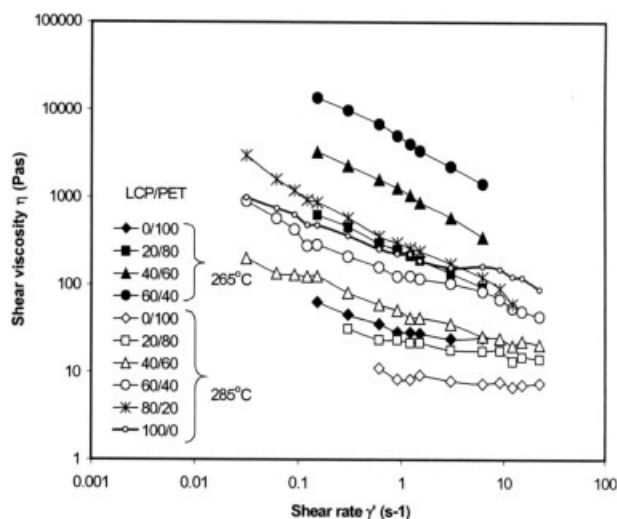


**Figure 5** Plots between the viscosity and shear rate for various LCP/PET blends.

composition of the blends significantly affects the viscosities at 265°C as shown in Figure 4. The variation in viscosity with the composition of blends at 285°C where LCP was in molten state was significantly less when compared with that of at 265°C. The curves represented by dotted lines show the viscosities of studied samples at very low shear rates. It is obvious from figure that shear viscosity corresponding to 80 : 20 LCP/PET blend shows a maxima that increases with lowering the shear rate at 285°C. The unblended LCP demonstrate a much lower value of viscosity at 285°C when compared with 80 : 20 LCP/PET blend. The viscosities of immiscible mixtures are the function of composition. The deviations from a rule of mixture in the form of maxima or minima are the indications of immiscibility of components.<sup>16</sup> The increased viscosity of such system may be attributed to the increased resistance offered by the dispersed phase. The increased volume fraction of the dispersed increases the viscosity. The dispersed particles form a temporary network and contribute a rise in viscosity.

The shear rate dependence of viscosity at two different temperatures; 265 and 285°C is shown in Figure 5 for various blends of LCP and PET along with the data of PET and LCP. At temperature 265°C the viscosity of PET was the least among the other samples within the range of studied shear rates. An increased loading of solid phase LCP in PET at 265°C increased the viscosity of the blend. The viscosity of samples decreased with the increase in shear rate. At temperature 285°C the viscosity of PET was the minimum when compared with all other blends and LCP and decreased with the shear rates. The viscosity increased with the addition of LCP in PET up to 80% of LCP in the blend. Interestingly, the viscosity of LCP was lower when compared with LCP/PET blends having higher volume fraction

of LCP than PET. The flow behavior of LCP is complex. The variation of viscosity with shear rate for LCP as reported<sup>5,8</sup> shows three viscosity regions. The poly-domain structure of LCP offers high resistance to flow to overcome domain structure in low stress region. Once materials starts flowing, progressive shear thinning is observed. The larger domains are broken down in smaller sizes with a large surface area and therefore higher viscosity is observed. The shear thinning in this region was attributed to size reduction of domains or to the defects in nematic phase.<sup>5,8</sup> At high shear rate molecules tend to orient in flow direction and hence viscosity reduces with shear rate. The LCP/PET blend has been reported as an immiscible blend.<sup>5,7</sup> The flow behavior of immiscible polymer blends is more complex because of the competition between deformation, breakup, coalesce of dispersed phase, and viscoelastic nature of phases. The viscosity of a system having deformable elastic particles suspended in Newtonian fluid can be estimated as per the following equation that correlate the effect of shear induced particle deformation and rotation in absence of Brownian effects;<sup>17</sup>

$$\eta = \eta_0[(1 + 2.5\phi) + \lambda_1^2\gamma^2(1 - 1.66\phi)]/(1 + \lambda_1^2\gamma^2)$$

where  $\lambda_1 = 3\eta_0/2G$ ,  $\eta_0$  viscosity of suspending medium,  $G$  is modulus of Hookean elastic particle, and  $\phi$  is volume fraction of droplet phase. This equation predicts shear-thinning viscosity that depends upon the volume fraction of droplet phase. In the present case when the deformation rate was very less, the LCP was present in spherical form in PET matrix and exhibited high viscosity of the system. On increasing the shear rate these spheres were deformed in flow direction and shear thinning was observed.

Figure 6 shows variation in shear viscosity with shear stress at temperatures 265 and 285°C for LCP, PET, and LCP/PET blends. In general a decrease in viscosity

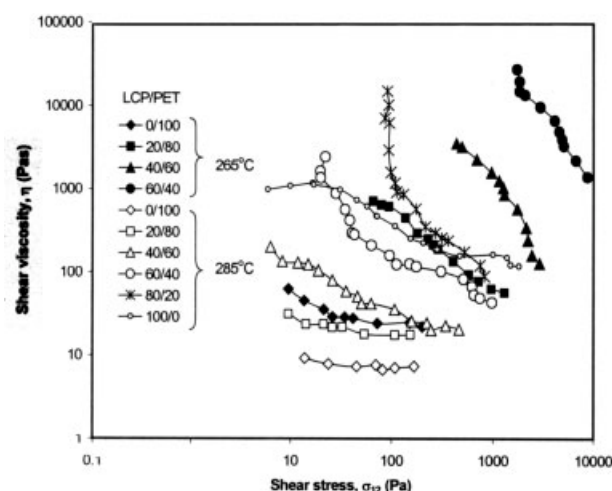


**Figure 6** Plots between shear stress and shear rate.

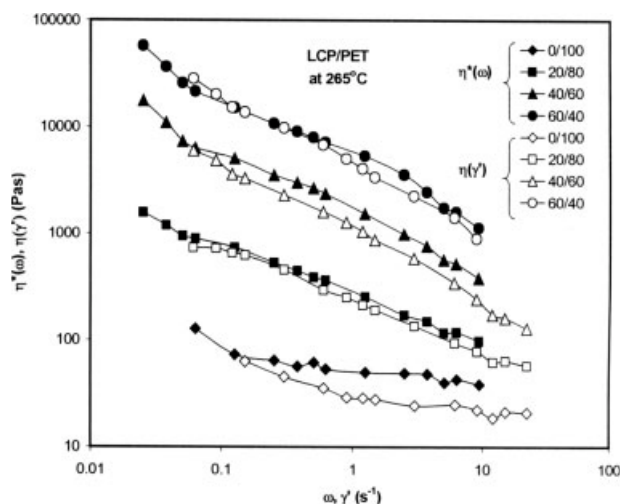


**Figure 7** Plots between  $\eta^*$  versus  $\omega$  and  $\eta$  versus  $\gamma'$  at 265°C.

with increased shear stress was observed. PET shows the least dependence on shear stress among the studied samples. As far temperature is concerned, there is almost ten times reduction in viscosity of PET at 285°C when compared with that of 265°C but the trend of curves is similar. The LCP shows nearly 100 times more the viscosity of PET at 285°C. The addition of LCP increased the viscosity of blend with varying the slope of the curve. The LCP/PET blends are extremely sensitive to shear stress almost showing the yield stress values of blends. The yield stress was observed in samples in which LCP is 60 wt % or more in the blend. It is evident that yield stress increased with the loading of LCP in PET. Such flow behavior is attributed to the formation of temporary network by the filler particles that become dense and stronger with the additional particles due to the increased interactions.<sup>18</sup>

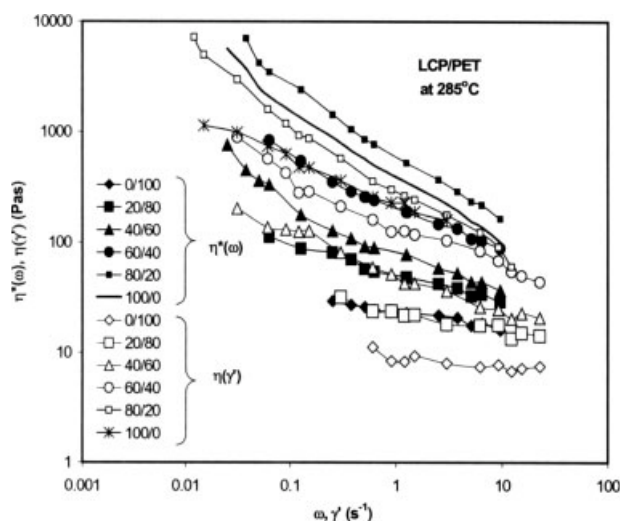


**Figure 8** Plots between  $\eta^*$  versus  $\omega$  and  $\eta$  versus  $\gamma'$  at 285°C.

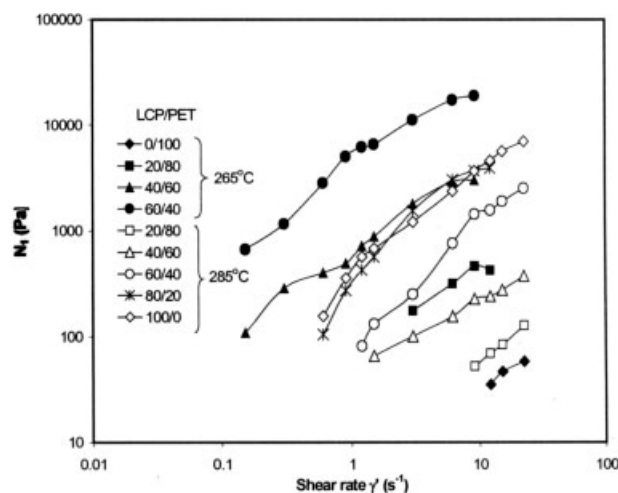


**Figure 9** Variation in first normal stress difference of LCP/PET blends with shear rate.

### Complex viscosity

The complex viscosity ( $\eta^*$ ) versus angular-frequency ( $\omega$ ) curves were compared with the steady state shear viscosity ( $\eta$ ) versus shear rate curves for PET and LCP/PET blends at temperatures 265 and 285°C as shown in Figure 7 and Figure 8 respectively. Many researchers have correlated  $\eta$  and  $\eta^*$  of polymer melts using Cox and Merz empirical law, according to which<sup>13</sup>

$$|\eta^*(\omega)| = \eta(\gamma') \quad \text{for } \omega = \gamma'$$

The value of  $|\eta^*|$  was comparatively higher than  $\eta$  in almost all cases; however the trends are similar. These results show that Cox-Merz law is not valid for the studied blend under applied test conditions. Generally  $\eta^*$  coincides well with  $\eta$  for polymer solutions and melts but shows higher values for dispersed system, which is attributed to special structures formed by the dispersed particles. Moreover the nature of both the polymers is different. The LCP was in solid state at 265°C and in anisotropic liquid form at 285°C. The dynamic conditions disturb the anisotropy of liquid LCP and additional energy was required to maintain a specified flow condition and might be resulted in higher values of  $\eta^*$ .

### First normal stress difference

First normal stress difference,  $N_1$ , in steady shear flow of a viscoelastic fluid may be considered as the amount of energy stored in viscoelastic liquid. The normal stress difference is expressed in terms of principal stresses. The  $N_1$  is plotted against shear rate at two different temperatures; 265 and 285°C for various compositions of LCP/PET blends and is shown in Figure 9. compared with  $N_1$  values of PET at 265°C, the LCP/

PET blend shows higher values.  $N_1$  is expected to decrease with the increased loading of nondeforming (rigid) filler in a molten polymer matrix because of the reduced recoverable elastic strain in the system. The increased value of  $N_1$ , as observed in the present study, suggests an increased elastic strain in the blend that may be attributed to either the presence of deformable LCP droplets or/and LCP-PET interactions. The increased value of  $N_1$  with the loading of particulates has been attributed to real shear rate acted on matrix and that is larger than the applied shear rate because the shear rate inside a rigid particle is zero.<sup>19–21</sup> In the present case the dispersed LCP particle experiences a torque because of the differential velocities of layers of suspending medium during sheared flow. This torque tries to rotate the particle. The tendency of rotation of particle shall disturb the flow. The disturbance would be minimum provided the particles are small in size and symmetric to the axis of rotation for example; spherical particles. An asymmetric particle, for example an elliptical particle, would exert a force while trying to rotate and a force perpendicular to the flow direction would be developed. This force is expected to be proportional to number of particles and the asymmetry of particles. It has been reported that the glass beads having diameter  $0.5 \times 10^{-2}$  to  $4 \times 10^{-2}$  mm suspended in Indopol L 100 did not respond in terms of  $N_1$  but the fibers of  $1.32 \times 10^{-2}$  mm radius and 12.7 mm length showed  $N_1$  values.<sup>19</sup> This mechanism explains the increased value of  $N_1$  on increased loading of LCP particles in the molten PET. On increasing LCP in PET number of LCP domains increased and few of those domains after coalescence make bigger droplets/particles with elliptical or guard shape.<sup>4</sup> This would increase the torque on these particles and their tendency to rotate would be resulted in the higher value of  $N_1$ .

The first normal stress difference and shear rate for polymer melts filled with small solid particles have been correlated as follows:<sup>22</sup>

$$N_1 = \sigma_{11} - \sigma_{22} = \{1 + Y[G^2(\lambda_1^2\gamma'^2 + 4/3\lambda_1^4\gamma'^4)]^{-1/2}\}2G\lambda_1^2\gamma'^2$$

$$\sigma_{11} - \sigma_{22} = 2G\lambda_1^2\gamma'^2 \quad \text{at high shear rates while } \gamma' \text{ is approaching to infinity}$$

$$\sigma_{11} - \sigma_{22} = 0 \quad \text{at low shear rates while } \gamma' \text{ is approaching to zero}$$

where  $\lambda_1$  is relaxation time,  $G$  is modulus,  $\lambda'$  is shear rate,  $Y$  is yield stress.  $N_1$  changes with shear rate from first order for textured materials<sup>23</sup> to second ordered for homogeneous polymers.<sup>24</sup> The shear-induced homogenization at high shear region causes changes in  $N_1$  depending upon the type of material. The dependency of  $N_1$  to second order of shear is

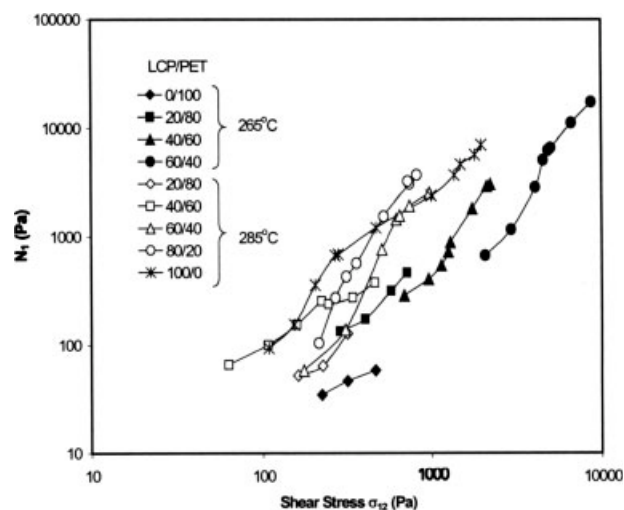


**Figure 10** Variation in first normal stress difference of LCP/PET blends with shear stress.

also attributed to shear induced alignment of micro domains structure.<sup>25</sup> The shear induced  $N_1$  for deformable elastic particles suspended in Newtonian fluid can be estimated as per following equations:<sup>17</sup>

$$N_1 = \sigma_{11} - \sigma_{22} = [8.33 \eta_0 \lambda_1 \gamma'^2 \phi] / (1 + \lambda_1^2 \gamma'^2)$$

where  $\lambda_1 = 3\eta_0/2G$ ,  $\eta_0$  is viscosity of suspending medium,  $G$  is modulus of Hookean elastic particle, and  $\phi$  is volume fraction of droplet phase. This equation predicts normal stress effect, which is proportional to volume fraction of droplet phase as was observed in present case.

The experimental values of  $N_1$  were plotted against the shear stresses as shown in Figure 10. PET exhibit lowest value of  $N_1$  whereas LCP shows much higher value. As far blends are concerned  $N_1$  decreased with increasing the LCP contents in the blend at 265°C. The trend was opposite at 285°C where the addition of LCP in the blend increased  $N_1$ . The slopes of the curves at 285°C are more than those at 265°C. It shows that shear stress sensitivity is higher in the blends containing molten LCP. The curves at 285°C as shown in Figure 10 have two stages. In first stage the slope of curves was more when compared with that of second stage and may be attributed to dominant elastic deformations of LCP droplets under applied shear that increased further with the volume fraction of LCP. The deformed droplets stored large amount of surface energy and consequently increased  $N_1$ . On further increase in shear stress the plastic deformation of LCP droplets took place and molecules aligned in flow direction, resulting in reducing the sensitivity of  $N_1$  on shear stress. The droplet deformation is controlled by mainly two parameters: the viscosity ratio and interfacial tension between the two fluids. In case the interfacial tension is negligible as compared to the viscosity effect, the deformed droplet



shall align in the flow direction. The droplet deformation criteria can be summarized as follows:<sup>10,26</sup>

If  $Ca^* < 0.1$ , droplet do not deform (deformation is negligible)

If  $0.1 < Ca^* < 1$ , droplet deform without break

If  $1 < Ca^* < 4$ , droplet deform, but break conditionally

If  $Ca^* > 4$  droplet deform affinely with the rest of matrix and extend into long stable filaments

Where reduced capillary number  $Ca^* = Ca/Ca_c$ .  $Ca = \text{Hydrodynamic stress/interfacial stress} = \eta_m \gamma R / \sigma$ , where  $\eta_m$  is matrix viscosity,  $\gamma$  the shear rate,  $R$  the drop radius,  $\sigma$  the interfacial tension, and  $Ca_c$  is critical capillary number beyond which the droplet can no longer sustain further deformation. Apart from the droplet deformation the surface erosion has been reported.<sup>27</sup> The relation between  $N_1$  and  $\sigma_{12}$  becomes quadratic and some times even higher near the forced-rubbery state region.<sup>28–30</sup> The similar observations were noticed here and found that LCP droplets were deformed on shearing and resulted in increased  $N_1$  with shear stress as shown in Figure 10.

## CONCLUSIONS

This study concludes as follows. The morphology and the shear viscosity of LCP/PET blends were composition dependent. A maxima was observed in viscosity versus composition plot corresponding to 80/20 LCP/PET blend. At low shear rates the LCP behaved like rigid particles at 265°C; however it was slightly deformed at higher shear rates and displayed shear thinning. First the normal stress difference  $N_1$  increased with the molten LCP content and then decreased with solid LCP content in the PET. The value of  $N_1$  increased with shear rate as well as with shear stress. At 285°C  $N_1$  varied with shear stress in two stages; the first stage demonstrated elastic deformation whereas second stage displayed dominant plastic deformation of LCP droplets in PET matrix.

One of the authors (SARH) is highly thankful to Dr. N. Ramakrishnan, Director RRL Bhopal for granting permission to publish this work. The author is also thankful to

Mr. R. S. Ahirwar, Scientist, RRL, Bhopal for his help in preparing the electronic-form of this manuscript.

## References

1. Kiss, G. *Polym Eng Sci* 1987, 27, 410.
2. Tjong, S. C. *Mater Sci Eng Rev* 2003, 41, 1.
3. Lin, Y. G.; Lee, H. W.; Winter, H. H. *Polymer* 1993, 34, 4703.
4. Shimizu, H.; Kitano, T.; Nakayama, K. *Mater Lett* 2004, 58, 1277.
5. Kyotani, M.; Kaito, A.; Nakayama, K. *Recent Res Dev Polym Sci* 1999, 3, 115.
6. Kyotani, M.; Kaito, A.; Nakayama, K. *J Appl Polym Sci* 1993, 47, 2053.
7. Kyotani, M.; Kaito, A.; Nakayama, K. *Polym Polym Compos* 1995, 3, 205.
8. Congswell, F. N. In *Recent Advances in Liquid Crystalline Polymers*; Chapoy, L. L., Ed.; Elsevier: New York, 1985; Chapter 10 (Fig. 8), p 172.
9. Marrucci, G. In *Thermotropic Liquid Crystal Polymer Blends*; La Mantia, F. P., Ed.; Technomic: Lancaster, PA, 1993; pp 43–58.
10. Song, C. H.; Isayev, A. I. *Polymer* 2001, 42, 2611.
11. Kataoka, T.; Ohnishi, S.; Kitano, T.; Nakama, K.; Takayama, H. *Rheol Acta* 1976, 15, 268.
12. Bird, R. B.; Armstrong, R. C.; Hassager, O. *Dynamics of Polymeric Fluid*, Vol. 1; Wiley: New York, 1977.
13. Yano, S.; Kitano, K. In *Handbook of Applied Polymer Processing Technology*; Cheremisinoff, N. P.; Cheremisinoff, P. N., Eds.; Marcel Dekker: New York, 1996.
14. Plochocki, A. P.; Dagli, S. S.; Andrews, R. D. *Polym Eng Sci* 1990, 30, 741.
15. Fortelny, I.; Zivny, A. *Polym Eng Sci* 1995, 35, 1872.
16. Meitz, D. W.; Yen, L.; Berry, G. C.; Markovitz, H. *J Rheol* 1988, 32, 309.
17. Goddard, J. D.; Miller, C. *J Fluid Mech* 1967, 28, 657.
18. Araki, T.; White, J. L. *Polym Eng Sci* 1998, 38, 616.
19. Han, C. D. *Multiphase Flow in Polymer Processing*; Academic Press: New York, 1981.
20. Tanaka, H.; White, J. L. *Polym Eng Sci* 1980, 20, 949.
21. Li, L. PhD Thesis, Kyoto University, Japan, 1989.
22. White, J. L. *J Non-Newtonian Fluid Mech* 1979, 5, 177.
23. Onuki, A. *Phys Rev A: At Mol Opt Phys* 1987, 35, 5149.
24. Ferry, J. D. *Viscoelastic Properties of Polymers*, 3rd ed.; Wiley: New York, 1980.
25. Takahashi, Y.; Noda, M.; Ochiai, N.; Noda, I. *Polymer* 1996, 37, 5943.
26. Huneault, M. A.; Shi, Z. H.; Utracki, L. A. *Polym Eng Sci* 1995, 35, 115.
27. Mighri, F.; Huneault, M. A. *J Appl Polym Sci* 2006, 100, 2582.
28. Brizitsky, V. I.; Vinogradov, G. V.; Isaev, A. I.; Padolsky, Y. Y. *J Appl Polym Sci* 1976, 20, 25.
29. Vinogradov, G. V.; Malkin, A. Y. *Rheology of Polymers*; Mir Publishers: Moscow, 1980; Chapter 4, p 324.
30. Czarnecki, L.; White, J. L. *J Appl Polym Sci* 1980, 25, 1217.